

Final Project Report

Contract/Grant Title: Development of High-Fill-Factor Large-Aperture Micromirrors for Agile Optical Phased Arrays

Contract/Grant #: FA9550-08-1-0292

Reporting Period: 1 June 2008 to 28 February 2010

Principal Investigator: Huikai Xie, University of Florida

Graduate research assistants:

Kemiao Jia, University of Florida

Sean R. Samuelson, University of Florida

Abstract

A new design of high-fill-factor (HFF) micromirror array (MMA) has been proposed, fabricated and tested. Optical-phased-array (OPA) beam steering based on the HFF MMA has also been demonstrated. This unique HFF MMA design consists of large sub-apertures (i.e., mirror pixels). The flatness of the mirror surface is provided by a 80 μ m-thick single-crystal silicon layer. The MMAs are fabricated using a single-wafer fabrication process without any wafer bonding, and the devices are surface-mountable right after the batch fabrication. A fabricated 4 \times 4 MMA achieves a combined optical aperture of 6.4mm \times 6.4mm with \sim 90% fill factor and $>\pm 25$ degree scan range in two axes at ± 4 V DC. A static piston of 320 μ m is achieved at less than 8V. The measured piston and rotation resonance modes are 247Hz and 320Hz, respectively. It is experimentally shown that the spot size from a rectangular aperture consisting of two consecutive sub-apertures is significantly reduced compared to that from a single sub-aperture when the phase difference between the two sub-apertures is electrically tuned to multiple 2π .

1. Background

High-fill-factor (HFF) micromirror arrays (MMAs) can form optical phased arrays (OPAs) for laser beam steering, free-space laser communications and directed energy applications. Ultra-large (>5 cm) combined optical apertures are desired to achieve high steering precision in long distances such as in airborne surveillance [1]. Existing HFF MMA solutions are either based on thin film micromachining technology such as SUMMiT-V or bulk silicon micromachining technology [2-5]. Thin film based MMAs can realize high fill factor but only with small sub-apertures [2]. One of the problems with small sub-apertures is that a large number of sub-apertures are required to achieve a large combined optical aperture. This demands stringent control of process variations as well as a tedious design of complex driving electronics. On the other hand, existing bulk-micromachined HFF MMAs have relatively large sub-apertures, but they need dedicated bonding/transfer steps, such as multiple wafer bonding/polishing [3], manual assembling [4] or flip-chip transferring [5], to integrate mirror plates to fragile actuators. Thereby, those MMAs have issues of high cost, low yield, and limited sub-aperture counts. So far, a simple, high-yield and scalable method of producing HFF MMAs is yet to be developed.

2. New Design Concept

We propose a single-wafer solution which can fabricate HFF MMAs with large, scalable apertures, and high yield. The concept of this design is developed from a previously-reported electro-thermal micromirror based on a folded dual S-shaped (FDS) bimorph actuator design [6]. The FDS bimorph actuator design is illustrated in Fig. 1a, where each actuator consists of two S-shaped bimorph beams. Each bimorph beam is made of two bimorph segments that have opposite layer structures. This FDS design can

REPORT DOCUMENTATION PAGE				<i>Form Approved</i> OMB No. 0704-0188	
Public reporting burden for this collection of information is estimated to average 1 hour per response, including the time for reviewing instructions, searching existing data sources, gathering and maintaining the data needed, and completing and reviewing this collection of information. Send comments regarding this burden estimate or any other aspect of this collection of information, including suggestions for reducing this burden to Department of Defense, Washington Headquarters Services, Directorate for Information Operations and Reports (0704-0188), 1215 Jefferson Davis Highway, Suite 1204, Arlington, VA 22202-4302. Respondents should be aware that notwithstanding any other provision of law, no person shall be subject to any penalty for failing to comply with a collection of information if it does not display a currently valid OMB control number. PLEASE DO NOT RETURN YOUR FORM TO THE ABOVE ADDRESS.					
1. REPORT DATE (DD-MM-YYYY) 26-02-2010		2. REPORT TYPE Final Report		3. DATES COVERED (From - To) Jun 01, 2008 - Feb. 28, 2010	
4. TITLE AND SUBTITLE Development of High-Fill-Factor Large-Aperture Micromirrors for Agile Optical Phased Arrays				5a. CONTRACT NUMBER	
				5b. GRANT NUMBER FA9550-08-1-0292	
				5c. PROGRAM ELEMENT NUMBER	
6. AUTHOR(S) Huikai Xie				5d. PROJECT NUMBER	
				5e. TASK NUMBER	
				5f. WORK UNIT NUMBER	
7. PERFORMING ORGANIZATION NAME(S) AND ADDRESS(ES) University of Florida Office of Engineering Research 339 Weil Hall Gainesville FL 32611				8. PERFORMING ORGANIZATION REPORT NUMBER	
9. SPONSORING / MONITORING AGENCY NAME(S) AND ADDRESS(ES) Air Force Office of Scientific Research 875 North Randolph Street Arlington, VA 22203-1768				10. SPONSOR/MONITOR'S ACRONYM(S)	
				11. SPONSOR/MONITOR'S REPORT NUMBER(S)	
12. DISTRIBUTION / AVAILABILITY STATEMENT Public Release					
13. SUPPLEMENTARY NOTES					
14. ABSTRACT A new design of high-fill-factor (HFF) micromirror array (MMA) has been proposed, fabricated and tested. Optical-phased-array (OPA) beam steering based on the HFF MMA has also been demonstrated. This unique HFF MMA design consists of large sub-apertures (i.e., mirror pixels). The flatness of the mirror surface is provided by an 80µm-thick single-crystal silicon layer. The MMAs are fabricated using a single-wafer fabrication process without any wafer bonding, and the devices are surface-mountable right after the batch fabrication. A fabricated 4×4 MMA achieves a combined optical aperture of 6.4mm×6.4mm with ~90% fill factor and >±25 degree scan range in two axes at ±4V DC. A static piston of 320µm is achieved at less than 8V. The measured piston and rotation resonance modes are 247Hz and 320Hz, respectively. It is experimentally shown that the spot size from a rectangular aperture consisting of two consecutive sub-apertures is significantly reduced compared to that from a single sub-aperture when the phase difference between the two sub-apertures is electrically tuned to multiple 2pi.					
15. SUBJECT TERMS					
16. SECURITY CLASSIFICATION OF:			17. LIMITATION OF ABSTRACT	18. NUMBER OF PAGES	19a. NAME OF RESPONSIBLE PERSON
a. REPORT	b. ABSTRACT	c. THIS PAGE			19b. TELEPHONE NUMBER (include area code)

achieve pure vertical displacement as well as compensate the lateral shift. A fabricated micro-mirror with four FDS actuators is shown in Fig. 1b. The cross-section view of the micro-mirror is shown in Fig. 1c, where the mirror plate is elevated above the substrate.

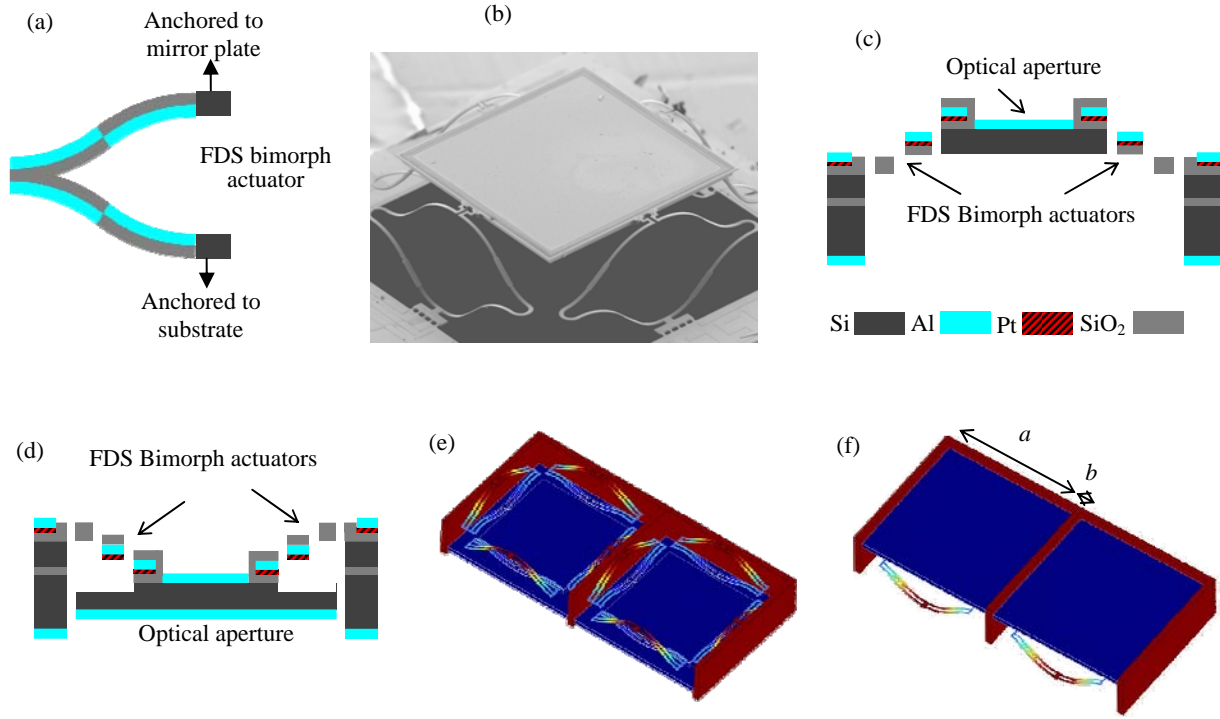


Figure 1 Design concept illustration. (a) Concept of the FDS actuator; (b) SEM image of the reported FDS micro-mirror; (c) Design of the reported FDS micro-mirror; (d) Design of the proposed new micro-mirror; (e) and (f) 3D models of the micro-mirror devices, illustrating hidden actuator and HFF.

The basic idea of our new micro-mirror design is to keep the mirror plate below the substrate surface, as illustrated in Fig. 1d. Meanwhile, the bottom surface of the mirror plate is used as the reflective mirror surface. So, the device will be flipped over upon actual use. Thus the bimorph actuators are effectively hidden underneath the mirror plate, resulting in high fill factor, as illustrated by the 3D models shown in Fig. 1e and 1f.

The initial deformation of the bimorphs can displace the mirror plate by several hundreds of microns. Therefore, the surface of the mirror plate can reach as far as to the bottom of the substrate. This condition ensures the mirror plate to have full mechanical protection from the silicon walls and at the same time minimizes the light blocking caused by the silicon walls. The silicon walls also act as heat sinks that thermally isolate the sub-apertures from each other. It is conceivable that an array of the micro-mirror shown in Fig. 1d can form a HFF MMA device with hidden actuators, as shown in Fig. 1e and Fig. 1f, from which the area fill factor of the MMA region can be estimated from geometry:

$$f = \left(\frac{a}{a+b} \right)^2 \quad (1)$$

in which a is the size of each sub-aperture, and b is the spacing between adjacent sub-apertures. Due to the thick silicon layer beneath the mirror plates, a can be in millimeter scale. The choice of b is subjected to several factors including the robustness of the silicon walls, manufacturability and process tolerances. In this design, $a=1.50\text{mm}$ and $b=100\mu\text{m}$, leading to a fill factor of 88%.

3. Device Fabrication

The fabrication and packaging process is illustrated in Figs. 2a~2e, in which $\text{SiO}_2/\text{Pt}/\text{SiO}_2/\text{Al}/\text{SiO}_2$ thin films are first sequentially deposited and patterned on the SOI wafer to form the bimorph actuators and bond pads (Fig. 2a). Then a front-side Si etch defines the sub-apertures (Fig. 2b), followed by backside Si/ SiO_2 etch and Al deposition (Fig. 2c) to form the mirror surfaces. Then, the Si under the bimorph actuators is undercut to release the sub-apertures (Fig. 2d). At last, simply by flipping the chip over, the actuators become hidden and the bonding pads are ready for surface-mounting even directly on a PCB with driving circuits (Fig. 2e). Due to the simplicity of this process, it achieved an overall yield of ~85% in this first trial run and the sub-aperture count can be easily scaled up.

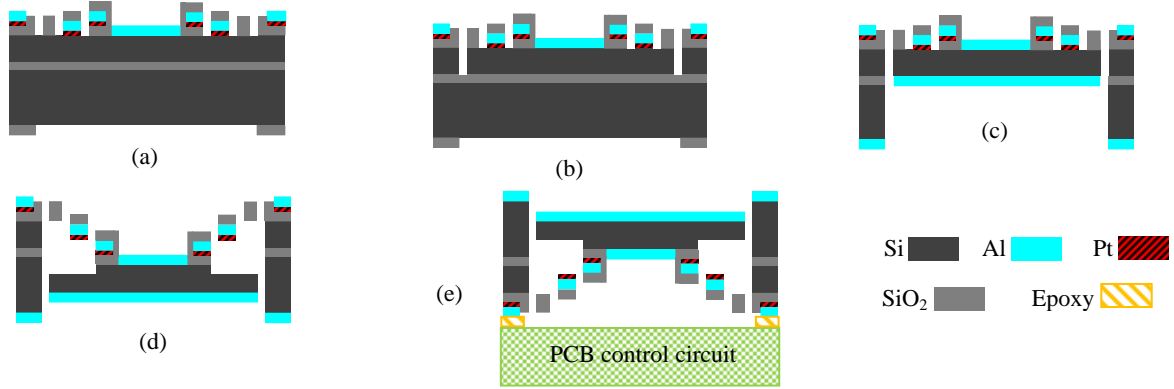


Figure 2 Cross sectional view of the device fabrication and packaging process.

Several SEM images of a fabricated 4×4 MMA device are shown in Fig. 3. The bird views of the device from the optical aperture side and from the actuator side are shown in Fig. 3a and Fig. 3d, respectively. The closed-up images of one sub-aperture and the hidden actuators are shown in Fig. 3b and Fig. 3c, respectively.

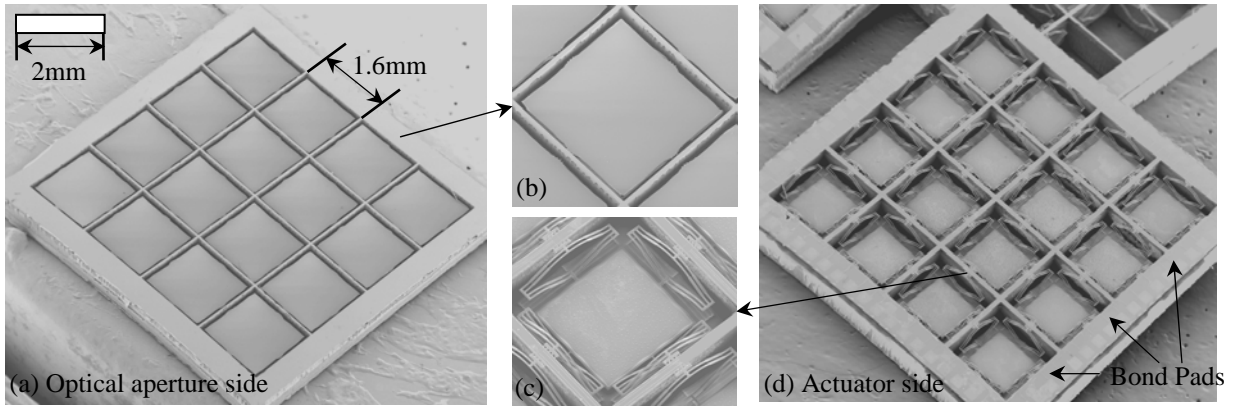


Figure 3 SEM images of the fabricated 4×4 MMA. (a) Bird view from the optical aperture side; (b) Close-up image of one sub-aperture; (c) Close-up image of the FDS bimorph actuator; (d) Bird view from the actuator side.

Following the packaging scheme in Fig. 2e, the surface-mount packaging of the 4×4 MMA device is done using an SEC-Model 850 Flip Chip Placement System. We first dispense Epo-Tek-H20E silver epoxy onto a PCB. Then, we align and position the PCB to the device and immediately cure the silver epoxy with a custom-made thin-film heater underneath. Fig. 4 shows the optical images of a surface mounted 4×4 MMA device wire-bonded in a DIP package, with one sub-aperture chosen to demonstrate the TTP capabilities.

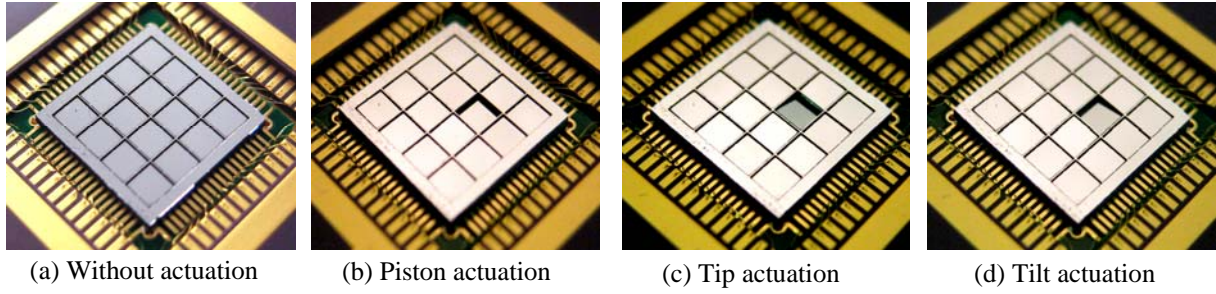


Figure 4 Optical images of a DIP packaged 4×4 MMA surface mounted on PCB.

4. Device Characterization

4.1 Static Response Measurement

The static piston response of a sub-aperture can be characterized by tracking the change of the vertical position of the mirror plate under a microscope. Fig. 5 shows the static measurement result of the piston actuation of one sub-aperture. A same dc voltage is applied to all four actuators of the sub-aperture to generate the piston displacement. It is measured that a piston stroke of $\sim 320\mu\text{m}$ can be realized at 8V dc. Meanwhile, the tilting angle of the mirror plate is initially $\sim 0.4^\circ$ at 0V and is increased to $\sim 1.0^\circ$ at the end of the actuation at 8V due to the resistance non-uniformity among the actuators. The static rotation actuation of one sub-aperture is characterized using a laser beam and a screen. A same dc voltage of 4V is applied to all four actuators while one pair of differentially varying voltages is superimposed on one opposing actuator pair. As shown in Fig. 6, optical deflection angles of $\sim \pm 30^\circ$ are achieved for both axes at a pair of 4V differential voltages. The slightly asymmetric characteristics between the two axes are also caused by the variations among the electrical resistances of the actuators.

4.2 Frequency Responses Measurement

The piston frequency response of the device is characterized using a Polytech laser vibrometer. A same periodic chirp signal of $6\text{V dc} + 0.2V_{\text{pp}} \text{ ac}$ is applied to one opposing actuator pair to excite the piston mode. The piston resonance peak is detected at 247Hz. The frequency response of the rotation resonance mode is measured using a laser and a screen. A same dc voltage of 4V superimposed by a $0.8V_{\text{pp}}$ sinusoidal differential ac signal pair is applied to one opposing actuator pair to excite the rotation mode. It is found that the rotation resonance occurs at 319Hz.

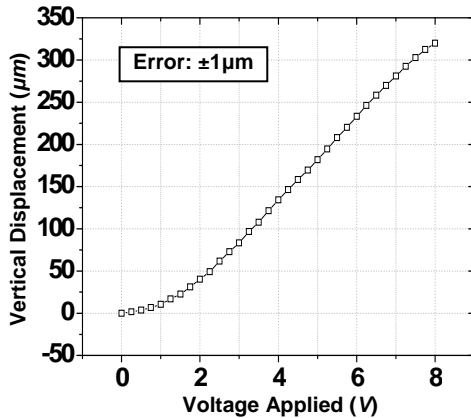


Figure 5 Measured static piston of one sub-aperture

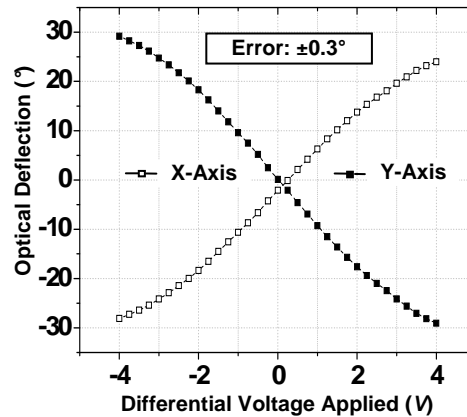


Figure 6 Measured static rotation of one sub-aperture.

4.3 Mirror surface Quality

The mirror surface quality is characterized using Wyko Vision optical profilometer. The mirror plate achieves a radius of curvature as large as -9 m (convex) at the center area. It is noticed that the radius of curvature is decreased to about 0.6 m (concave) at ~ 0.2 mm to the edge due to the thinner Si support.

5. Optical Phased Array Experiment

For OPA applications, the sub-apertures of the MMA device must have individual accessibility and accurate dual-axis steering capability. To demonstrate the individual accessibility, a He-Ne laser beam is expanded and collimated using two lenses and is incident on the MMA device. Using each reflected light spot as an image pixel, different letters are formed by controlling the actuators. The schematic setup and the result of this experiment are shown in Fig. 7.

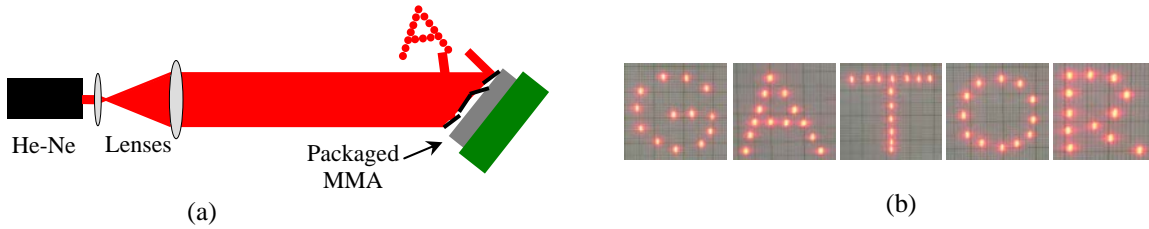
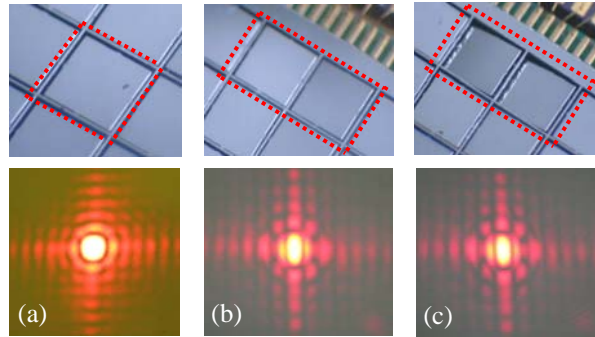


Figure 7 (a) Setup of the individual accessibility experiment. (b) Letters scanned using the sub-apertures.

As an OPA beam steering unit, the large combined optical aperture formed by the micro-mirrors must steer the laser beam as if it is reflected from a single large mirror. Therefore, to demonstrate this accurate angular steering capability, we can study the far-field pattern of the reflected beam from adjacent sub-apertures. First, a far-field pattern by illuminating just a single sub-aperture is obtained, which is a symmetric square spot as shown in Fig. 8a. Then by illuminating a rectangular aperture consisting of two consecutive sub-apertures, a far-field diffraction pattern with a reduced spot size is obtained, as shown in Fig. 8b, which closely resembles the calculated wave front profile when the phase difference between the two sub-apertures equals zero or $2n\pi$. Under this condition, when compared with the diffraction pattern of a single sub-aperture in Fig. 8a, it is evident that the 2×1 rectangular aperture reduces the spot size in the longer edge. If a 2×2 square aperture is used, the spot size will be reduced in both directions. The reduced spot can be steered to as much as 30° with little size change, as shown in Fig. 8c.

Figure 8 Diffraction patterns of (a) one mirror pixel; (b) two consecutive mirror pixels with a 0° tilt angle; and (c) two consecutive mirror pixels with a 15° tilt angle.



The above two experiments demonstrate the MMA device's random access and precise angular control capabilities, which are the preliminary requirements for MMAs to be used in OPA laser steering systems. More characterizations and experiments will be carried out and more sophisticated driving electronics will be developed to demonstrate the full OPA functions of large micro-mirror arrays.

CONCLUSION

A new design and fabrication method of electro-thermal HFF MMAs with large mirror plates has been demonstrated. The MMA devices have low driving voltage and large scanning range. The fabrication process is based on single SOI wafers without additional bonding/ transfer steps, leading low cost and high yield. A 4×4 MMA is fabricated up to now but the sub-aperture count can be easily scaled up. The millimeter-size sub-apertures make this type of MMA devices particularly suitable for long-distance laser steering applications, for which the preliminary capabilities have been experimentally demonstrated. Our future work will focus on developing a fully functional OPA unit based on this design and further improving the fabrication process, mirror surface quality and device robustness.

REFERENCES:

- [1] P. F. McManamon, *et al.*, *Proceedings of IEEE*, vol. 97, 2009.
- [2] J.-c. Tsai and M. C. Wu, *Journal of Micro-electro-mechanical Systems*, vol. 15, pp. 1209-1213, 2006.
- [3] M. Kim, *et al.*, *Journal of Micromechanics and Microengineering*, vol. 19, pp. 035014, 2009.
- [4] V. Milanovic, G. A. Matus, and D. T. McCormick, *Journal of Selected Topics in Quantum Electronics*, vol. 10, pp. 462-471, 2004.
- [5] P. J. Gilgunn and G. K. Fedder, *Hilton Head Workshop, Hilton Head Island*, pp. 10-13, 2008.
- [6] K. Jia, S. Pal, and H. Xie, *Journal of Micro-electro-mechanical Systems*, vol. 18, pp. 1004-1015, 2009.